Wind and Structures, *Vol. 24, No. 5 (2017) 405-430*
DOI: https:// doi.org/10.12989/was.2017.24.5.405

Dynamic analysis of long-span cable-stayed bridges under wind and traffic using aerodynamic coefficients considering aerodynamic interference

Wanshui Han[1a], Huanju Liu[*1], Jun Wu[1b], Yangguang Yuan[1c] and Airong Chen[2d]

[1]*Department of Bridge Engineering, Chang'an University, Xi'an, Shanxi, 710064, China*
[2]*Department of Bridge Engineering, Tongji University, Shanghai, 200092, China*

(Received May 10, 2016, Revised April 15, 2017, Accepted April 29, 2017)

Abstract. The aerodynamic characteristics of vehicles are critical to assess vehicle safety and passenger comfort for vehicles running on long span bridges in a windy environment. However, in previous wind–vehicle–bridge (WVB) system analysis, the aerodynamic interference between the vehicle and the bridge was seldom considered, which will result in changing aerodynamic coefficients. In this study, the aerodynamic coefficients of a high-sided truck on the ground (ground case) and a typical bridge deck (bridge deck case) are determined in a wind tunnel. The effects of existent structures including the bridge deck and bridge accessories on the high-sided vehicle's aerodynamic characteristics are investigated. A three-dimensional analytical framework of a fully coupled WVB system is then established based on the finite element method. By inputting the aerodynamic coefficients of both cases into the WVB system separately, the vehicle safety and passenger comfort are assessed, and the critical accidental wind speed for the truck on the bridge in a windy environment is derived. The differences in the bridge response between the windward case and the leeward case are also compared. The results show that the bridge deck and the accessories play a positive role in ensuring vehicle safety and improving passenger comfort, and the influence of aerodynamic interference on the response of the bridge is weak.

Keywords: wind–vehicle–bridge system; aerodynamic interference; vehicle stability; critical wind speed; bridge response

1. Introduction

The southeast coastal region of China has more than 18,000 km of coastline and many bays and islands. To cross over bays and connect the mainland and islands, many sea-crossing bridges have been constructed or are in the building process, such as the Hangzhou Bay Tunnel Bridge, the East China Sea Bridge, the Qingdao Bay Bridge, the Zhoushan Islands Link Project, and the Hong Kong-Zhuhai-Macao Bridge. One of the primary variable loads for long-span bridges is the wind

∗Corresponding author, Ph.D., E-mail: huanjull@163.com
[a] Professor, E-mail: hws_freedom@163.com
[b] Associate Professor, E-mail: jun.wu@chd.edu.cn
[c] Ph.D., E-mail: yuanyg31@163.com
[d] Professor, E-mail: a.chen@tongji.edu.cn

http://www.techno-press.org/?journal=was&subpage=8 ISSN: 1226-6116 (Print), 1598-6225 (Online)

force. A strong wind force not only threatens the safety of the bridge but also has a significant impact on vehicle driving safety and passenger comfort. Thus, it is crucial to assess the safety of the bridge passing vehicles and the driving comfort under various wind and traffic conditions.

A series of studies on coupled wind–vehicle–bridge (WVB) systems (Xu and Guo 2003, Cai and Chen 2004, Cheung and Chan 2010, Li *et al*. 2012) have been carried out during the last decade. However, the aerodynamic coefficients of road vehicles involved in previous WVB system analyses seldom consider the aerodynamic interference between the vehicle and the bridge. The majority of WVB system analyses adopted the aerodynamic coefficients for high-sided vehicle obtained by Baker (1991a, b), whereas some researchers used the aerodynamic coefficients of typical vehicle models obtained by wind tunnel tests (Ma *et al*. 2015, Han *et al*. 2015a) according to the vehicle's aerodynamic configuration. However, little did the above studies consider the interaction of the aerodynamic forces between the road vehicles and the bridge. The aerodynamic force coefficients of vehicles under wind load depend on not only the shapes of vehicles but also those of the bridge deck and the corresponding accessory structures. The presence of the bridge deck would cause the wind flow around the vehicle to be more complicated compared with the case in which the same vehicle is on the ground. Accordingly, the aerodynamic characteristics may change significantly for a vehicle on the bridge. To investigate the influence of the bridge deck and the corresponding accessory structures (i.e., protection rail) on the aerodynamic characteristic of vehicle models, some researchers have developed a series of experimental setups to measure the aerodynamic coefficients of vehicles and the bridge in a wind tunnel (Suzuki *et al*. 2003, Zhu *et al*. 2012, Han *et al*. 2013) considering the aerodynamic interference between the vehicles and the bridge. Others have addressed the same problems using numerical simulation methods (Bettle *et al*. 2003). However, the aerodynamic coefficients in most studies above were not further inputted into the WVB system analysis, which makes it difficult to investigate vehicle stability and passenger comfort through the vehicle's response and to study the influence of aerodynamic interference on the bridge's response. With the deepening of research, some leading scholars (Han *et al*. 2014, 2015, Wang *et al*. 2015) have begun to study effects of aerodynamic interference on the response of bridges and vehicles based on WVB system, and achievements which are significant for the subsequent studies have been made. However the research mentioned above has not further studied the influence of aerodynamic interference on the safety of vehicles.

A lot of researches (Guo and Xu 2006, Li *et al*. 2012, Chen and Cai 2004, Ma *et al*. 2015) have been carried out in vehicle safety. Based on previous WVB system, the response of vehicle on the bridge under crosswind has been analyzed, and the vehicle safety has been evaluated, some have even given the critical wind speed and the critical vehicle speed. These researches are significant for improving the level of bridge management. However, the vehicle aerodynamic coefficients adopted in these studies seldom consider the aerodynamic interference between vehicle and bridge, which makes it difficult to accurately assess vehicle stability and passenger comfort.

The overall research progress in this paper can be divided into the four following sections. The first section obtains the aerodynamic coefficients of the high-sided vehicle in a wind tunnel, which can be used to consider the aerodynamic interference between the vehicle and the bridge (bridge deck case). Wind tunnel tests of the same vehicle on the ground (ground case) are also conducted for further comparison. Second, a three-dimensional analysis framework of a fully coupled WVB system based on the finite element method is developed. Third, the aerodynamic coefficients of the bridge deck case and the ground case are both used as input parameters for the WVB system analysis. Fourth, the coupled vibration of WVB systems are calculated to obtain the vehicle responses such as the acceleration and interaction forces (moments). The time history, maximum

value and root mean square (RMS) of the bridge displacement and acceleration can also be obtained by the WVB systems. Based on the analytical results, the vehicle safety and passenger comfort are further assessed according to the defined criteria, and then the influence of aerodynamic interference on the bridge response is also studied.

2. Aerodynamic coefficients measurement considering aerodynamic interference

2.1 Bridge information

In this paper, the Hangzhou Bay Sea-Crossing Bridge is taken as the prototype. The meteorological survey reveals that the region of Hangzhou Bay is dominated by a humid subtropical monsoon climate and experiences hazardous climate frequently. Furthermore, the narrow pipe effect is formed because of the trumpet-shaped topography of Hangzhou Bay, which causes the local weather patterns of this region to be more complex (Xu and Shi 2002). The North Channel Bridge of the Hangzhou Bay Sea-Crossing Bridge is a box-girder cable-stayed bridge with a span arrangement of 70+160+448+160+70 m comprising double-plane stay cables and twin towers as shown in Fig. 1(a). Its deck, a closed streamline cross-section of a single box with two wind-fairings, is 3.5 m high and 37.1 m wide and carries a dual three-lane highway (see Fig. 1(b)). The six lanes are identified as lanes 1–6 in a sequence from the windward lane to the leeward lane. There are 112 stay cables in total, and the stay cables are composed of parallel steel-wire strands. The distance between adjacent stay cables is 15 m. The main tower is 181.3 m high and of a diamond shape, including the upper, middle, and bottom columns with a tie beam between the legs.

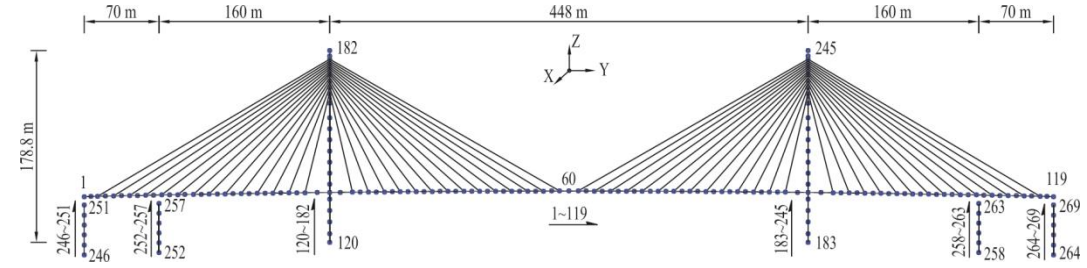

(a) Structural arrangement and positions of wind speed simulation points

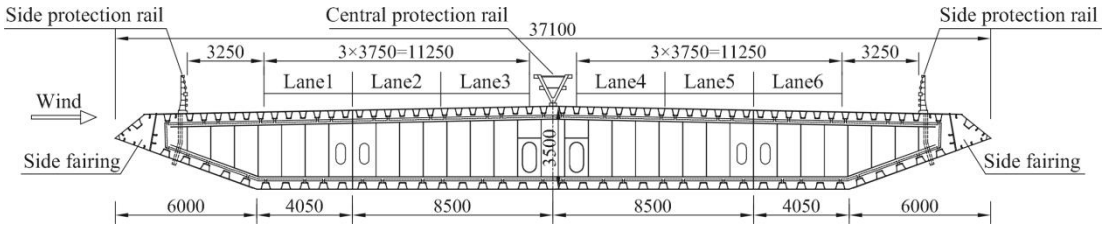

(b) Cross section of bridge deck (Unit: mm)

Fig. 1 Configuration of the Hangzhou Bay Bridge

2.2 Bridge deck and vehicle models

Post-disaster investigations have revealed that overturning accident was the most common type of wind-induced vehicle accidents, and the corresponding vehicle types were mainly high-sided road vehicles (Baker and Reynolds 1992). Therefore, the high-sided road vehicle was always selected as the sample vehicle type in previous studies. In this study, the high-sided road vehicle is again chosen as the analytical object.

The geometric scale of the vehicle model and the bridge model was adopted as 1:30 according to the size of the working section of the wind tunnel and the capacity of the force balance. The deck sectional model with a width of 1.24 m and a length of 1.3 m was designed. Fig. 2 gives the detailed dimensions of the vehicle model. To measure the vehicle on different lanes under various wind yaw angles, the force balance measurement technique was chosen to measure the aerodynamic forces on the vehicle model. Because the vehicle model required high stiffness and light weight considering the capacity of the force balance, according to Zhu's experience (Zhu *et al*. 2012), high-quality wood plates with stiffeners were selected to form the vehicle chassis, and high-density plastic foam was used to form the vehicle body.

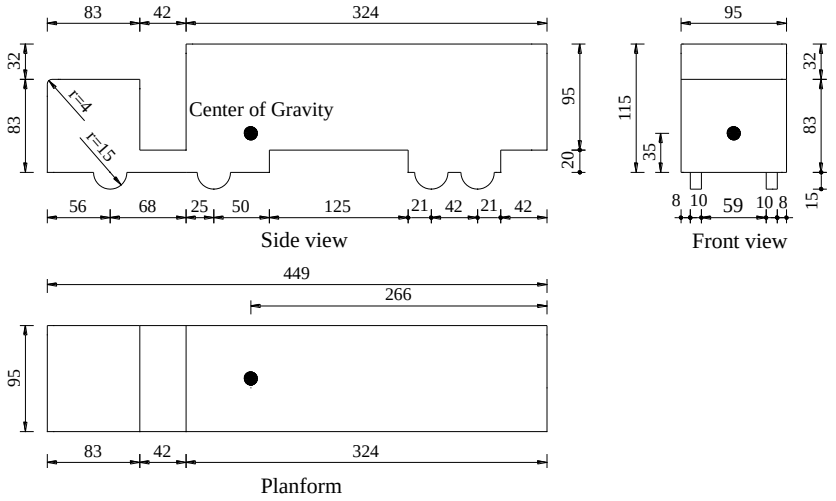

Fig. 2 High-sided vehicle model of 1:30 scale (unit: mm)

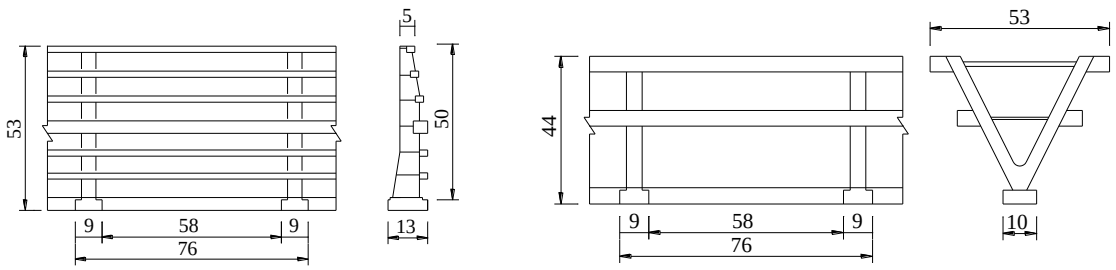

Fig. 3 Configurations and dimensions of rail models (unit: mm)

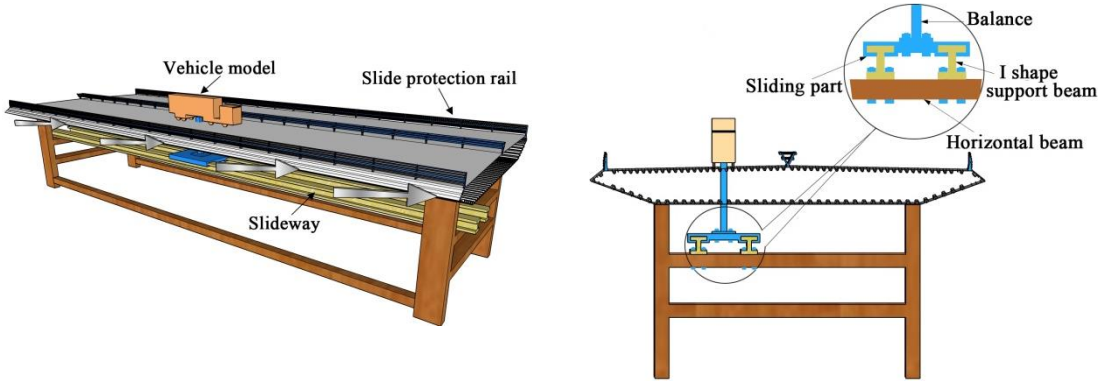

Fig. 4 Schematic diagram of testing system

The influence of the bridge deck and accessory structures on the aerodynamic forces of the vehicle was the main focus in this study. Therefore, the deck exterior appearance including the side and central protection rails was modeled considering geometric similarity. The configurations and dimensions of the side and central protection rails of the deck model can be observed in Fig. 3. Their ventilation ratios were typically approximately 75% and 79%, respectively.

2.3 Experimental setup

The experimental setup developed in this study can measure the aerodynamic coefficients of a vehicle interfered by the bridge deck. The bridge model was supported by four square steel posts firmly connected by one longitudinal and two horizontal square steel beams, which can provide high stiffness for the deck model to ensure the measurement accuracy of aerodynamic forces on vehicle models. A high-frequency force balance of six components was used to measure the aerodynamic forces and moments on the vehicle model. The top side of the force balance was connected with the vehicle, and the bottom side of the force balance was supported by a thick steel plate with two grooves on each side. The thick steel plate was connected with two parallel I-shape steel beams through grooves, which were fixed by the upside horizontal square steel beam as shown in Fig. 4. The force balance was fixed in the middle of deck model when the deck case was studied. The test frames and the models were installed on the turntable of the wind tunnel, which can rotate with the table together to vary the wind yaw angle. The wheel sets of the vehicle model were not allowed to touch the bridge deck surface during tests with a gap of approximately 1 mm. The measurement ranges of the balance were $100\,N$ to $200\,N$ and $10\,N\cdot m$ to $50\,N\cdot m$ for forces and moments, respectively. Before the wind tunnel test, the measurement accuracy of the balance was calibrated, which showed that the maximum measurement deviation of the fore and moment was smaller than 0.5%.

2.4 Wind environment above bridge deck

Before the measurement of vehicle aerodynamic coefficients, the wind environment test above the bridge deck model without the vehicle model was carried out first in the TJ-3 wind tunnel of

the State Key Laboratory for Disaster Reduction in Civil Engineering at Tongji University in China.

As shown in Fig. 5, the outermost windward lane (lane 1) and leeward lane (lane 6) without vehicles were chosen to measure the mean velocity profile above the bridge deck via anemometer. Because the height of a high-sided vehicle is usually no more than 4.5 m, the maximum measuring height of the wind velocity was set to 4.5 m, and the vertical measuring coordinate was set to 0.15, 0.30, 0.45, 0.60, 0.90, 1.20, 1.50, 1.80, 2.40, 3.00, 3.60, 4.50 m (Zhu *et al*. 2012). The wind direction is normal to the bridge deck, and the experimental wind speed was set to 8.5 m/s.

Fig. 5 shows the profiles of mean wind speed over lane 1 and lane 6 of the bridge deck without vehicles measured from wind tunnel tests. The vertical coordinate is the prototype height over the deck surface (z), whereas the horizontal coordinate is the mean wind speed $U(z)$ above the deck at z. It can be observed in Fig. 5 that the mean wind speed is significantly reduced by the existence of the bridge deck and the sheltering effect of the windward side and central protection rails. Moreover, the mean wind speeds below the height of approximately 2 m for windward lane 1 and approximately 3 m for leeward lane 6 are smaller than the experimental wind speed of 8.5 m/s, whereas the mean wind speeds above these two heights are greater than 8.5 m/s.

To assess the sheltering effects in different lanes quantitatively, a pressure-equivalent wind speed is introduced and defined as follows (Zhu *et al.* 2012)

$$U_{eq}^2 = \frac{1}{z_r}\int_0^{z_r} u^2(z)dz \tag{1}$$

where z_r is a reference height set as 4.5 m in consideration of the height of vehicles. Based on the measurement results of wind profiles displayed in Fig. 5, the reduced factors of equivalent wind speeds (U_{eq}/U) of lanes 1 and 6 are 0.930 and 0.834, respectively. The results show that the reduction in side forces in the leeward lane is greater than that in the windward lane, which can be attributed to the increase in wake height of the side protection rails along the wind direction and the additional sheltering effect of the central protection rails.

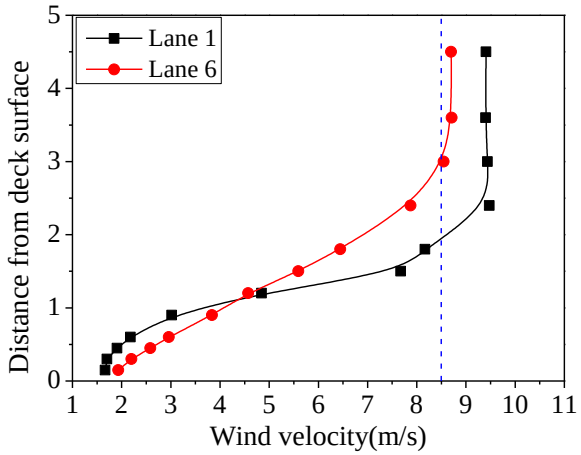

Fig. 5 Mean wind speed profiles above lane 1 and lane 6

2.5 Test results of vehicles on bridge deck

Wind tunnel tests on the vehicle model of in the ground case and the bridge deck case were carried out in the TJ-1 wind tunnel of the State Key Laboratory for Disaster Reduction in Civil Engineering at Tongji University in China. The TJ-1 wind tunnel is a boundary layer wind tunnel, with a working section of 1.8 m in width, 1.8 m in height and 14 m in length. The achievable mean wind speed in the tunnel ranges from 0.5 to 30 m/s, and the wind speed could be adjusted continuously.

To simulate the road vehicles in the wind tunnel experiments, the geometric similarity between the scale model and the full-size vehicle must first be satisfied. In addition, true dynamic similarity also requires a matched Reynolds number

$$\mathrm{Re} = \frac{U\mathrm{H}}{\nu} \tag{2}$$

where U is the flow velocity, H is the height of the vehicle center of gravity from the ground (or the bridge deck surface in this study), and ν is the kinematic viscosity of air.

The wind tunnel tests of aerodynamic coefficients of the high-sided truck on the ground have been conducted extensively by Baker (1991) and Zhu (2012). The Reynolds numbers in their studies range from 0.40×10^5 to 2.4×10^5. The Reynolds numbers in previous wind tunnel tests are much lower than those in the full-scale flow owing to the limitations in the size and the maximum flow speed of the wind tunnel. The aerodynamic coefficients obtained from Zhu's test and Baker's tests have a variation pattern similar to that of the wind yaw angle overall. Furthermore, Zhu determined the aerodynamic coefficients of road vehicles over a bridge deck compared with the aerodynamic coefficients of road vehicles on the ground. However, the tested wind yaw angles of vehicle models on the bridge deck range from 60° to 90°, and the parameters are inadequate for further input to the WVB system analysis for investigating the vehicle stability and passenger comfort. In this study, The Reynolds number of the vehicle model is 0.40×10^5. The vehicle models of the ground case and the bridge case were both tested in static conditions (i.e., without vehicle movement) at a wide range of wind yaw angles from 0° to 90° with intervals of 10°. All test cases were performed in a smooth flow with a mean wind speed of 10 m/s. The turbulence intensity in the smooth flow tests was measured to be less than 1.0%. The sampling frequency was 200 Hz, and the number of sampling points was 8192.

In the ground case, the vehicle model was mounted on the turntable above the wind tunnel floor. The wheel sets of the vehicle model were not allowed to touch the wind tunnel floor, with a gap of approximately 1 mm. Given the effect of the boundary layer on the wind tunnel, there are differences between the aerodynamic forces measured in the wind tunnel and those on the ground. The aerodynamic coefficients of the ground case measured in a wind tunnel test should be amended as recommended by the Society of Automotive Engineers (SAE 1993). The disturbances of the boundary layer mainly include the following three aspects: correction of the clog effect, correction of the ground boundary layer effect and correction of the horizontal buoyant force. Detailed information on these three corrections can be found in the previous research by the authors (Ma *et al*. 2015). In the bridge deck case, the influence of the wind tunnel on the aerodynamic coefficients mainly results from the increased wind speed due to the clog effect of the vehicle and the bridge model. Therefore, real-time wind speed measurement was conducted at the wind tunnel cross section of the vehicle model, and the mean wind speed was then corrected.

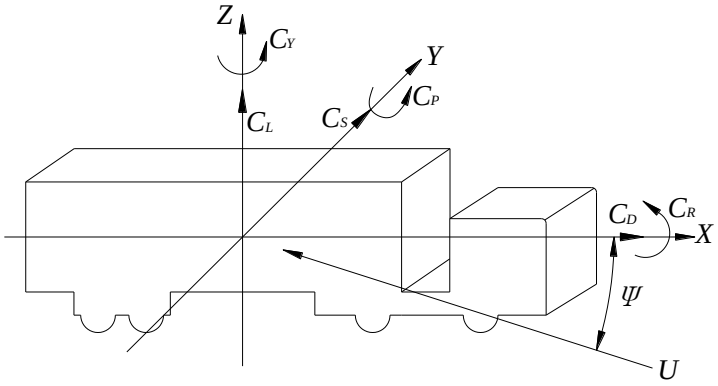

Fig. 6 Sign convention for aerodynamic forces of the vehicle

The positive directions of the forces and moments acting on a road vehicle are depicted in Fig. 6, and the aerodynamic coefficients are defined by the following equations

$$\begin{cases} C_D(\psi)=\dfrac{F_x}{0.5\rho U^2 A_r}; & C_S(\psi)=\dfrac{F_y}{0.5\rho U^2 A_r}; & C_L(\psi)=\dfrac{F_z}{0.5\rho U^2 A_r} \\ C_R(\psi)=\dfrac{M_x}{0.5\rho U^2 A_r h_v}; & C_P(\psi)=\dfrac{M_y}{0.5\rho U^2 A_r h_v}; & C_Y(\psi)=\dfrac{M_z}{0.5\rho U^2 A_r h_v} \end{cases} \tag{3}$$

where F_x, F_y, F_z, M_x, M_y and M_z are the drag force, side force, lift force, rolling moment, pitching moment, and yawing moment acting on the vehicle, respectively; $C_D(\psi)$, $C_S(\psi)$, $C_L(\psi)$, $C_R(\psi)$, $C_P(\psi)$ and $C_Y(\psi)$ are the drag force coefficient, side force coefficient, lift force coefficient, rolling moment coefficient, pitching moment coefficient, and yawing moment coefficient, respectively, which are functions of the yaw angle ψ; A_r (unit: m^2) is the reference area, which is the frontal project area of a vehicle without wheels; h_v (unit: m) is the reference height, which is normally taken as the height of the vehicle center of gravity above the ground; ρ is the air density of 1.225 kg/m^3; and U (unit: m/s) represents the wind speed of uniform flow.

The six aerodynamic coefficients of the high-sided truck on the bridge deck and ground are depicted in Figs. 7(a)-7(f) for the wind yaw angles ranging from 0° to 90°. The aerodynamic coefficients of the vehicle on the ground are also shown in Fig. 7 for comparison.

The conclusions on the aerodynamic coefficients of the vehicle can be drawn from Figs. 7(a)-(f).

1) Side force coefficients: It can be observed that the side force coefficients for the vehicle on the ground and on the windward lane have the same tendency: the coefficients increase with increasing yaw angle. The side force coefficients for the vehicle on the leeward lane increase rapidly with increasing yaw angle from almost zero at 0° to 40°, and then they show a stage of decreasing with increasing yaw angle from 50° to 90°. The side force coefficients for the vehicle on the bridge deck are significantly less than those on the ground owing to the reduction effect of the side and central protection rails. Moreover, the side force coefficients for the vehicle on the leeward lane are smaller than those on the windward lane.

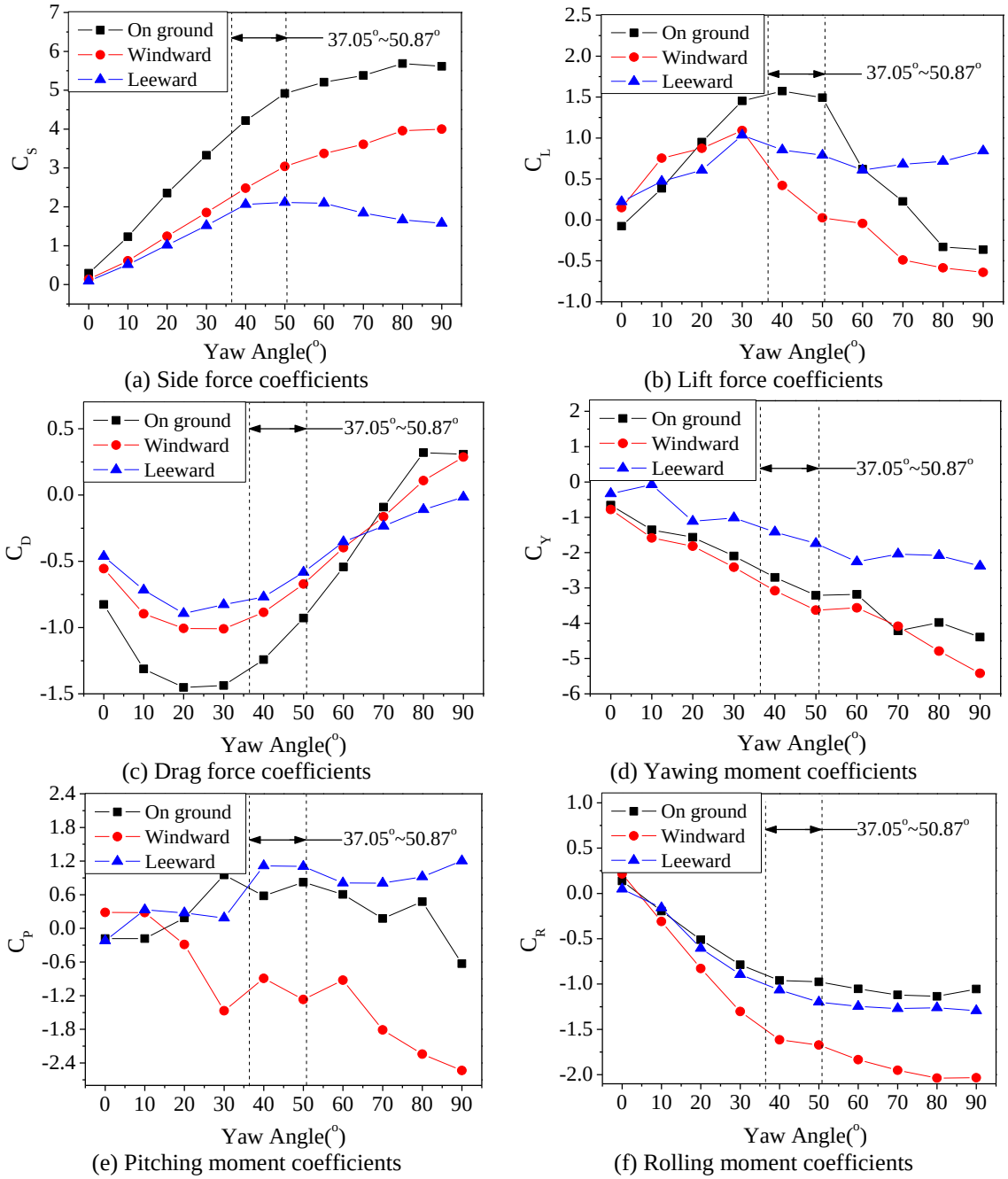

Fig. 7 Comparison of aerodynamic coefficients of a high-sided truck on the ground and windward and leeward lanes of the bridge

2) Lift force coefficients: Whether the vehicle is on the ground, on the windward lane or on the leeward side of the bridge, the overall trends of lift force coefficients first increase and reach their maximum values and then decrease. The yaw angle corresponding to the maximum values on the ground is between 30° and 50°, whereas those on the windward and leeward lanes of the bridge are approximately 30°. The lift force coefficients on the leeward lane at high yaw angles are positive, whereas those on windward lanes may be negative.

3) Drag force coefficients: The drag force coefficients for the vehicle on the ground and on the windward lane of the bridge vary remarkably with yaw angle, and their sign changes from negative to positive at a yaw angle of approximately 70°. The drag force coefficients for the vehicle on the leeward are always negative. The minimum (maximum absolute) drag force coefficients of the three types of vehicles appear at a yaw angle of approximately 20°.

4) Yawing moment coefficients: The yawing moment coefficients for the vehicle under the three different conditions increase with increasing yaw angle. Compared with the yawing moment coefficients on the ground, those on the leeward lanes decrease in the presence of the bridge deck, whereas those on the windward lanes do not change remarkably.

5) Pitching moment coefficients: The pitching moment coefficients on the leeward lane and on the ground have almost the same trend, but they are completely different from those on the windward lane. The pitching moment coefficients on the windward lane are negative, and the absolute values increase with increasing yaw angle.

6) Rolling moment coefficients: The rolling moment coefficients for the vehicle under the three different conditions increase sharply with increasing yaw angles from 0° to approximately 40° and then increase slowly with increasing yaw angles ranging from 40° to 90°. The rolling moment coefficients on the windward lane are far greater than those on the ground, whereas those on the leeward lane are slightly greater than those on the ground. The possible reason is that the shielding effect of the rails on the lower part of the vehicles will lead to a significant reduction of the mean wind speed of the lower parts and the increasing action point of the resultant side force on the vehicle.

The general findings can be drawn from the comparisons of the six aerodynamic coefficients corresponding to the ground case and the bridge deck case.

Owing to the sheltering effect of the side and central protection rails, the side force and drag force coefficients on the bridge deck become smaller than those on the ground.

The rolling moment coefficients on the bridge deck are greater than those on the ground, especially for those on the windward lane. The reason is that the action point of the resultant side force on the vehicle increases owing to the shielding effect of the side and central protection rails to the lower part of the vehicles.

The overall trends of the influence of the bridge deck on the lift force coefficient, the pitching moment coefficient, and the yawing moment coefficient are not very obvious.

3. General fully coupled wind–vehicle–bridge (WVB) interaction model

To investigate vehicle safety, passenger comfort on the bridge and the effects of aerodynamic interference on the bridge response, the WVB interaction model established by the authors (Wang and Han 2014, Ma and Han 2015, Han *et al.* 2015a, Han *et al*. 2015b) was introduced to predict the dynamic performance of the bridge and of vehicles running on bridges in a wind environment. The bridge and the vehicle are regarded as two subsystems, and the equations of motion of the

WVB system that consider excitations from wind and road roughness can be expressed in the following form

$$\begin{bmatrix} \mathbf{M}_b & 0 \\ 0 & \mathbf{M}_v \end{bmatrix} \begin{Bmatrix} \ddot{u}_b \\ \ddot{u}_v \end{Bmatrix} + \begin{bmatrix} \mathbf{C}_b & 0 \\ 0 & \mathbf{C}_v \end{bmatrix} \begin{Bmatrix} \dot{u}_b \\ \dot{u}_v \end{Bmatrix} + \begin{bmatrix} \mathbf{K}_b & 0 \\ 0 & \mathbf{K}_v \end{bmatrix} \begin{Bmatrix} u_b \\ u_v \end{Bmatrix} = \begin{Bmatrix} \mathbf{F}_{bg} + \mathbf{F}_{bst} + \mathbf{F}_{bbu} + \mathbf{F}_{bse} + \mathbf{F}_{bv} \\ \mathbf{F}_{vg} + \mathbf{F}_{vst} + \mathbf{F}_{vb} \end{Bmatrix} \tag{4}$$

where M, C and K are the mass, damping and stiffness matrices, respectively; u represents the displacement vector; subscripts v and b denote the vehicle and bridge, respectively; F_{bg}, F_{bst}, F_{bbu}, F_{bse} and F_{bv} are the self-weights of the bridge, the static wind force, the buffeting force, the self-excited force and the wheel–bridge contact force acting on the bridge, respectively; F_{vg}, F_{vst} and F_{vb} are the self-weights of the vehicle, the quasi-static wind forces and the wheel–bridge contact forces acting on the vehicle, respectively.

The bridge and vehicle systems are established independently, and the nonlinear iteration method is chosen to solve the above differential equations, which makes a full-interaction analysis of bridges under busy traffic and wind very efficient.

The wind action on a running vehicle includes the static and dynamic load effects. The quasi-static wind forces on vehicles are adopted because a transient type of the force model is unavailable (Baker 1994). The total aerodynamic forces and moments acting on the vehicle can be determined using the relative wind velocity with respect to the vehicle (Cai and Chen 2004),

$$U_r(x_v,t) = \sqrt{\left\{\left(U + u(x_v,t)\right)\cos\beta + v(x_v,t)\sin\beta + U_v\right\}^2 + \left\{\left(U + u(x_v,t)\right)\sin\beta + v(x_v,t)\cos\beta\right\}^2} \tag{5}$$

$$\psi = \arctan\left[\frac{\left(U + u(x_v,t)\right)\sin\beta + v(x_v,t)\cos\beta}{\left(U + u(x_v,t)\right)\cos\beta + v(x_v,t)\sin\beta + U_v}\right] \tag{6}$$

where U is the mean wind velocity component; U_v is the velocity of the vehicle; x_v is the position of the vehicle, which is located between nodes i and j of the bridge deck at any time t; $u(x_v,t)$ and $v(x_v,t)$ are the turbulent wind velocity component of the vehicle in and vertical direction for mean wind flow direction. β is the attack angle of the wind with respect to the vehicle, which is the angle between the wind direction and the direction in which the vehicle is moving.

The turbulent wind speed $u(x_v,t)$ and $v(x_v,t)$ acting on the vehicle is not a function merely of time but also position because the instantaneous position of a moving vehicle is time variant. The longitudinal fluctuating wind speeds acting on the vehicle should be compatible with the wind speeds used in determining wind forces acting on the bridge deck. Therefore, if the position of the vehicle x_v at any time t is located between nodes i and j of the bridge deck, $u(x_v,t)$ and $v(x_v,t)$ used to determine wind forces on the vehicle are determined by (Han *et al.* 2015a)

$$u(x_v,t) = \left(\frac{x_v - x_i}{x_j - x_i}\right)u_j(t) + \left(\frac{x_j - x_v}{x_j - x_i}\right)u_i(t) \tag{7}$$

$$v(x_v,t)=\left(\frac{x_v-x_i}{x_j-x_i}\right)v_j(t)+\left(\frac{x_j-x_v}{x_j-x_i}\right)v_i(t) \tag{8}$$

where x_i and x_j are the x-coordinates of node i and node j, respectively; $u_i(t)$ and $u_j(t)$ are the horizontal turbulent wind speed at a given time t. $v_i(t)$ and $v_j(t)$ are the vertical turbulent wind speed at a given time t.

4. Analysis and result

4.1 Input parameters

The modified spectral representation method is used to simulate the whole bridge wind field for the Hangzhou Bay Bridge, and the wind speed distributions of the simulated points are shown in Fig. 1(a). The simulated points are chosen to coincide with the discrete nodes of the bridge finite element model. The horizontal wind spectrum is adopted in Kaimal's form (1972), whereas the vertical spectrum is in the form presented by Lumley and Panofsky (1964), and the adopted coherence function is in Davenport's form (1972).

The WVB system mentioned previously can be used to calculate the response of the bridge and the vehicle when random traffic flow travels across the bridge. However, because only the aerodynamic parameters of the high-sided truck were measured by the wind tunnel test, a vehicle platoon composed of a single model of high-sided truck is adopted for the traffic flow. When the distance between vehicles is greater than the length of the vehicle itself, the aerodynamic interference between vehicles can be neglected (Wu 2008). Thus, a vehicle platoon consisting of 10 high-sided trucks with a spacing of 20 m was constructed. The starting point of the first vehicle is set at the position of -3105 m to ensure a time period of 138 s to stabilize the motion of the bridge in the wind field before the vehicle enters the bridge. Fig. 8 presents the operating diagram for a windward vehicle platoon on the bridge. "Excellent" road roughness corresponding to class "A" defined by ISO (1995) was considered because the Hangzhou Bay Bridge has been periodically maintained.

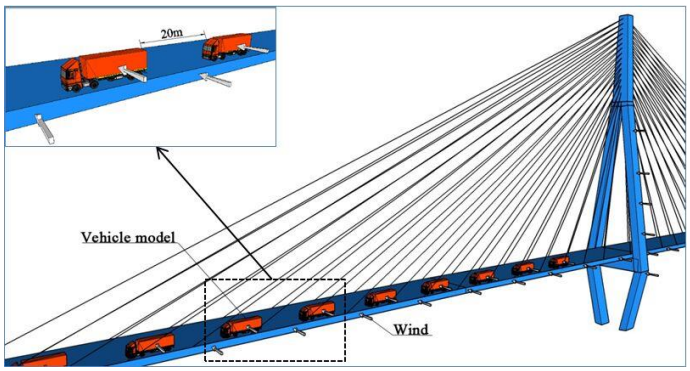

Fig. 8 The operating diagram for the windward vehicle platoon on the bridge

4.2 Safety analysis for high-sided vehicle

4.2.1 Vehicle instability situations

Based on Baker (1991), Cheung and Chan (2010) redeveloped a set of vehicle instability criteria from the stepwise free body of the vehicle–bridge system, which is more realistic and suitable for random traffic moving on the bridge, so this paper chooses it as the standard of the accident. "Potential vehicle instability" situations will occur when the following mechanisms are formed: 1) the vehicle is traveling on the bridge normally, and one of the tire reactions falls to zero (an overturning accident); 2) the rotational moment caused by the wind loading is greater than the resistant rotational moment caused by the frictional forces at all contact points (rotation accident); 3) the sum of the lateral frictional forces available on all tires is less than the total lateral loading (wind loads) acting on the vehicle body (sideslip accident).

4.2.2 Turbulent wind velocity profile and the instantaneous attack angle

A high-sided truck on the windward outermost lane is selected in the following analysis. When the mean speed is 20 m/s, the turbulent wind velocity profile acting on the vehicle is determined as shown in Fig. 9(a) by using the dynamic interpolation technique of wind velocity proposed in Eq. (7).

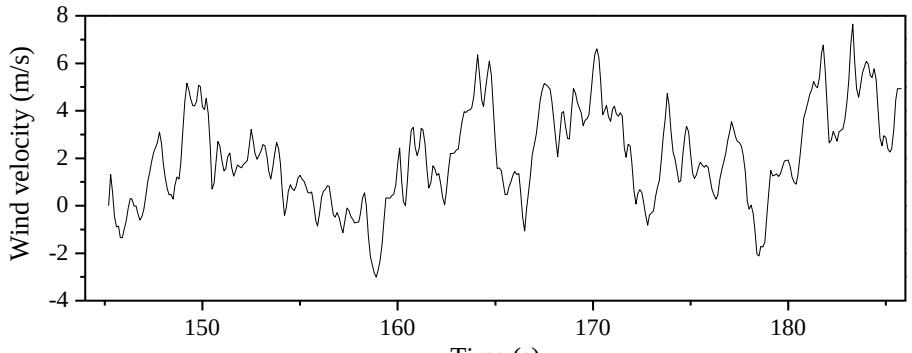

(a) Turbulent wind velocity profile acting on the vehicle

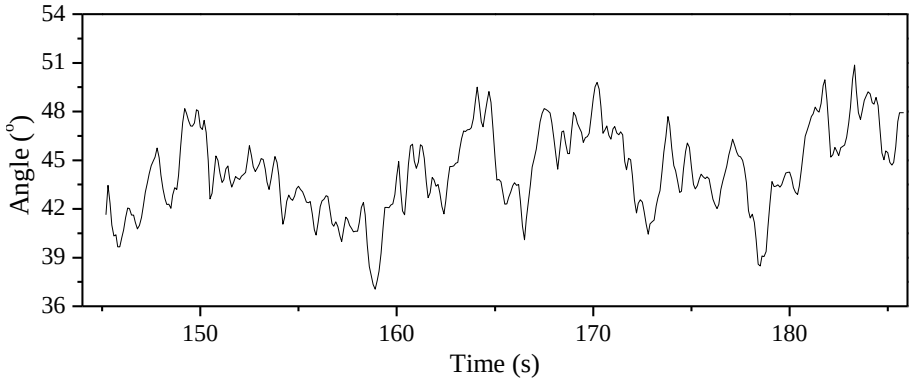

(b) The instantaneous angle between the wind direction and the vehicle movement direction

Fig. 9 Turbulent wind velocity profile and the instantaneous attack angle

The total equivalent wind forces acting on the vehicle can be determined from the horizontal wind force, which is composed of the mean wind and the turbulent wind components, and the wind force generated from the moving action of the vehicle. The instantaneous angle between the total resultant equivalent wind direction and the vehicle movement direction is shown in Fig. 9(b). It can be found that the instantaneous angle ranges from 37.05° to 50.87° when the vehicle speed is 80 km/h and the mean wind speed is 20 m/s. After the attack angle is determined, the aerodynamic coefficients of the vehicle can be interpolated according to measured coefficients as shown in Fig. 7. The aerodynamic forces acting on the vehicle body can then be obtained.

4.2.3 Aerodynamic force

Three different cases are chosen to investigate the effect of the aerodynamic interference on the vehicle safety and passenger comfort, namely the ground case, leeward case and windward case, which refers to that the vehicles run on the bridge adopting aerodynamic coefficient of the high-sided truck running on the ground, the windward side and the leeward side of the bridge. Under those three different situations, the side force, lift force, drag force, yawing moment, pitching moment and rolling moment of the vehicle in crosswind can then be calculated and extracted directly from the numerical WVB analysis model established in the previous section.

However, as known from the previous standard of accidents, the vertical force at the contact point is the criterion for judgment of an overturning accident. If the vertical force on any tire falls to zero, an overturning accident will occur. The results of different trial runs suggest that the overturning instability condition is most likely to be initiated at the windward rear wheel. Thus, the vertical force on the windward rear wheel is taken as the criterion for judgment of an overturning accident. The vertical interaction forces in windy environments are influenced by the following three types of aerodynamic forces. The first force is the side force acting on the vehicle's geometric center, which can produce an overturning moment, and the second force is the rolling moment directly acting on the rigid body of the vehicle. The above two forces can reduce the vertical interaction forces for the windward wheels and increase those for the leeward wheels. The third force is the aerodynamic lift force which can increase or reduce the vertical interaction forces for all wheels uniformly. The overturning moment is resisted by the vehicle self-weight. Thus, the side force, rolling moment and lift force on the windward rear wheel will be analyzed to judge an overturning accident.

For a vehicle moving in a straight line under a crosswind field, the non-coincidence between the center of crosswind and the gravity center of the vehicle will cause a yawing moment, which can interact with the rolling moment, leading to the occurrence of a rotation accident. A sideslip accident occurs mainly because of the side force (wind loads) acting on the vehicle. Each resistance force (moment) of the two types of accidents is provided by the friction force, the availability of which depends on the frictional coefficient and the vertical reaction force on the wheels. As known, the friction coefficient is constant, so each resistance force (moment) is determined by the vertical reaction force. From previous analysis, the vertical reaction force is related to the side force, rolling moment, and lift force. Thus, the side force, rolling moment, and lift force should be analyzed to judge a rotation accident and side-slipping accident.

In summary, the side force, lift force, yawing moment, and rolling moment are closely related to the three types of accidents. Therefore, the following figures present the time history of the side force, rolling moment, lift force and yawing moment when the vehicle speed is 80 km/h, the mean wind speed is 20 m/s, and the attack angle is 90°.

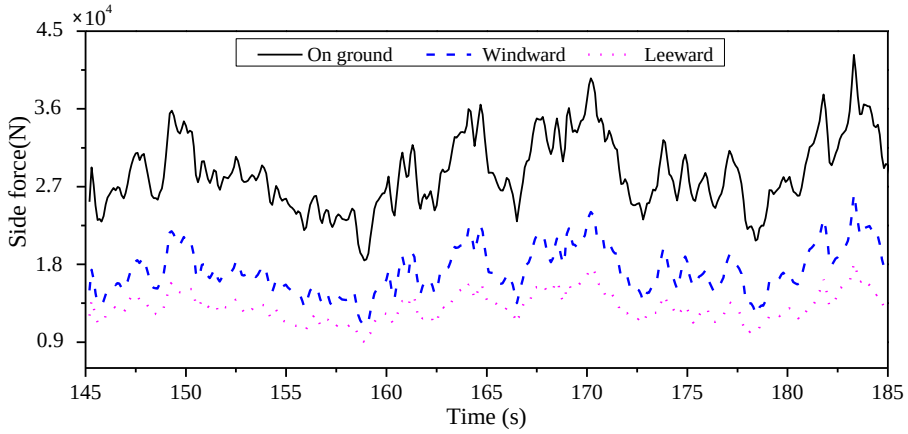

(a) Side force

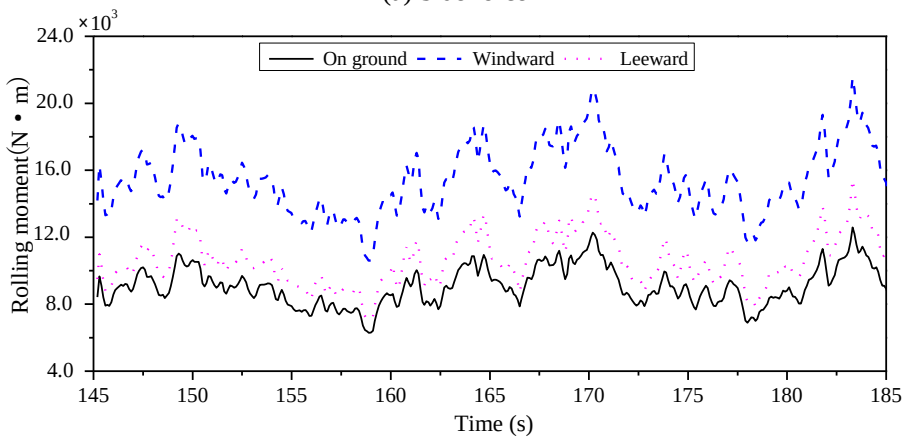

(b) Rolling moment

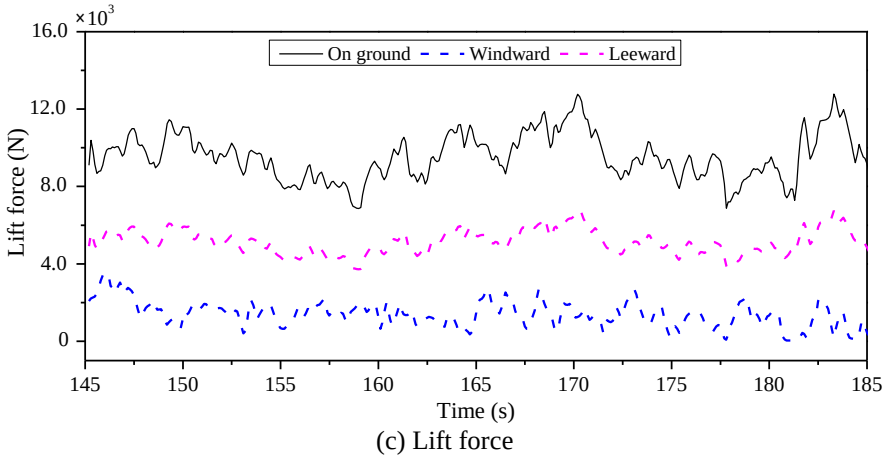

(c) Lift force

Continued-

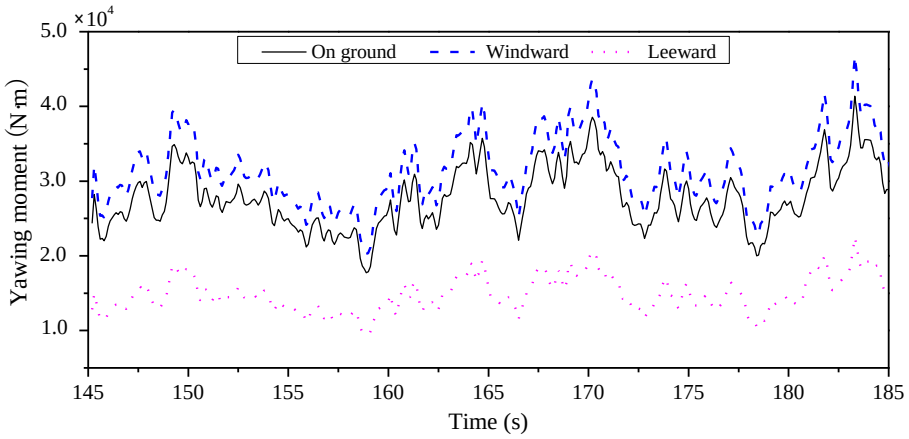

(d) Yawing moment

Fig. 10 Comparison of aerodynamic forces of high-sided vehicle on the ground, windward and leeward cases

For a vehicle moving in a straight line under a crosswind field, the non-coincidence between the center of crosswind and the gravity center of the vehicle will cause a yawing moment, which can interact with the rolling moment, leading to the occurrence of a rotation accident. A sideslip accident occurs mainly because of the side force (wind loads) acting on the vehicle. Each resistance force (moment) of the two types of accidents is provided by the friction force, the availability of which depends on the frictional coefficient and the vertical reaction force on the wheels. As known, the friction coefficient is constant, so each resistance force (moment) is determined by the vertical reaction force. From previous analysis, the vertical reaction force is related to the side force, rolling moment, and lift force. Thus, the side force, rolling moment, and lift force should be analyzed to judge a rotation accident and side-slipping accident.

In summary, the side force, lift force, yawing moment, and rolling moment are closely related to the three types of accidents. Therefore, the following figures present the time history of the side force, rolling moment, lift force and yawing moment when the vehicle speed is 80 km/h, the mean wind speed is 20 m/s, and the attack angle is 90°.

Fig. 10 shows the comparisons of aerodynamic forces under different vehicle aerodynamic coefficients in the ground case and bridge case. According to Eq. (3), it can be known that the aerodynamic force (moment) and the corresponding aerodynamic coefficients are linearly related. When the vehicle speed is 80 km/h and the mean wind speed is 20 m/s, the instantaneous angle ranges from 37.05° to 50.87°. Comparing Fig. 10 with Fig. 7, the sequences of aerodynamic coefficients are the same as the aerodynamic forces (moments). For example, in Fig. 7(a), when the abscissa axis is between 37.05° and 50.87°, the side force coefficient of the ground case is the greatest, followed by those of the windward and then the leeward cases. The difference between the ground case and the windward case is greater than that of the windward and leeward cases. The side force diagram in Fig. 10 reflects the same regularity, and the same is true for the lift force, yawing moment, and rolling moment with corresponding aerodynamic coefficients.

4.2.4 Safety analysis for high-sided truck considering aerodynamic interference

When the vehicle travels at 80 km/h and the mean wind speed is 20 m/s, the attack angles range from 37.05° to 50.87°. The vertical interaction forces on the windward rear wheel, the total lateral resisting forces and the resisting yawing moment were separately calculated using the WVB system described previously. Based on the established vehicle instability situations, the calculation results were separately compared with 0, the side force and the rotation moment to determine whether the vehicle instability situation occurs under the ground case, windward case and leeward case.

Based on the vehicle instability situations, an overturning accident will occur if the windward rear wheel reactions fall to zero. Fig. 11 shows the vertical interaction forces of the windward rear wheel comparisons under different vehicle aerodynamic coefficients in those three situations. From Fig. 11, the following can be found:

1) From the observation of Fig. 11, the vehicle is not subjected to any overturning instability condition because the vertical interaction forces are greater than zero throughout the vehicle journey. The vertical interaction forces adopting the aerodynamic coefficients on the ground are apparently smaller than those of the aerodynamic coefficients on the windward lane and on the leeward lane. This indicates that a vehicle adopting the aerodynamic coefficients on the ground is prone to suffer overturning instability. Furthermore, the interaction forces adopting the aerodynamic coefficients on the windward lane are slightly greater than those for the wheels on the leeward lane.

2) The vertical interaction forces are directly associated with the aerodynamic coefficients adopted in the calculation. When the vehicle travels at 80 km/h under a mean wind speed of 20 m/s, the instantaneous attack angles are between 37.05° and 50.87° as discussed earlier. It can be found in Fig. 7(a) that the side force coefficients corresponding to the attack angles ranging from 37.05° to 50.87° on the ground are significantly greater than those on the windward lane and on the leeward lane. This can cause the windward wheels to have a smaller vertical interaction force if adopting the aerodynamic coefficients on the ground compared with adopting the aerodynamic coefficients in the other two cases.

3) Because the side force coefficients (Fig. 7(a)) and the rolling moment coefficients (Fig. 7(f)) of the vehicle on the windward lane are both greater than those on the leeward lane, the vertical interaction forces corresponding to aerodynamic coefficients on the windward lane should be smaller than those on the leeward lane if the lift force coefficients for both cases are identical. However, the upward lift force coefficients on the leeward lane are greater than those on the windward lane. This will lead to an additional decrease in the vertical interaction forces for wheels on the leeward lane relative to those on the windward lane. Therefore, there is only a slight difference between the vertical interaction forces on the windward lane case and the leeward lane case, although the aerodynamic coefficients have distinctive differences between the two cases.

To judge the occurrence of the vehicle sideslip instability, the total lateral resisting frictional forces on the tires are plotted against the total lateral sideslip forces corresponding to three different aerodynamic coefficient input modes in Fig. 12.

1) Based on the observation of Fig. 12, the vehicle sideslip instability conditions corresponding to the three different cases are summarized as follows: the sum of the lateral resistance forces available on all tires is greater than the total lateral wind loads acting on the vehicle body in all three cases, so the vehicle is not subjected to any sideslip accident.

2) The side forces are determined by the side force coefficients. As shown in Fig. 7(a), the side force coefficients on the ground are the greatest, those on the windward lane are second, and those

in the leeward case are the least. The same relationships also exist in the side forces as shown in Fig. 12. As shown in Fig. 7(b), the lift force coefficients on the ground are the greatest, those on the leeward lane are second, and those in the windward case are the least. The positive value indicates a lift force on the vehicle, which will reduce the vertical interaction force. Therefore, the vertical interaction force adopting coefficients on the windward lane are the maximum, those on the leeward lane are second, and those in the ground case are the least. As mentioned before, the resisting frictional force is equal to the multiplication of the vertical interaction force and the friction coefficient. Thus, the total horizontal frictional forces present a trend similar to that of the vertical interaction force.

3) If using the aerodynamic coefficients measured on the ground, the vehicle is prone to suffer sideslip instability compared with the other two cases. The reason is that the side forces are the greatest, whereas the sideslip instability resistance force (total horizontal frictional force) is the least among the three cases. The instability probability of the other two cases is close, which can be observed from the relative relationships of the total lateral sideslip forces and the total lateral resisting frictional force.

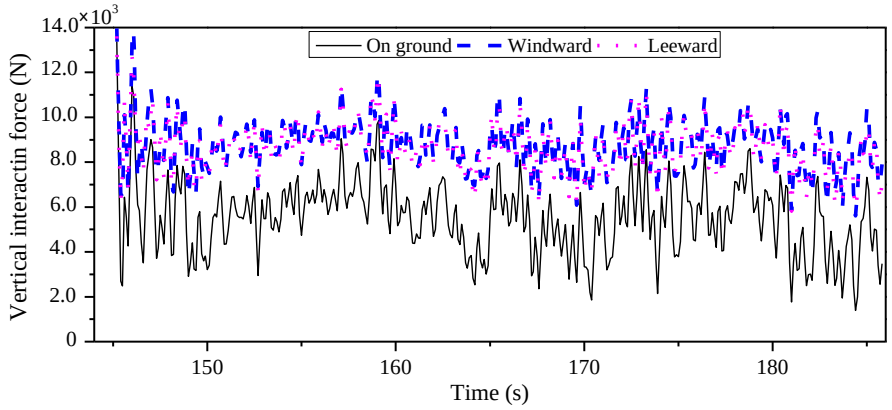

Fig. 11 Vertical reaction forces under three different cases

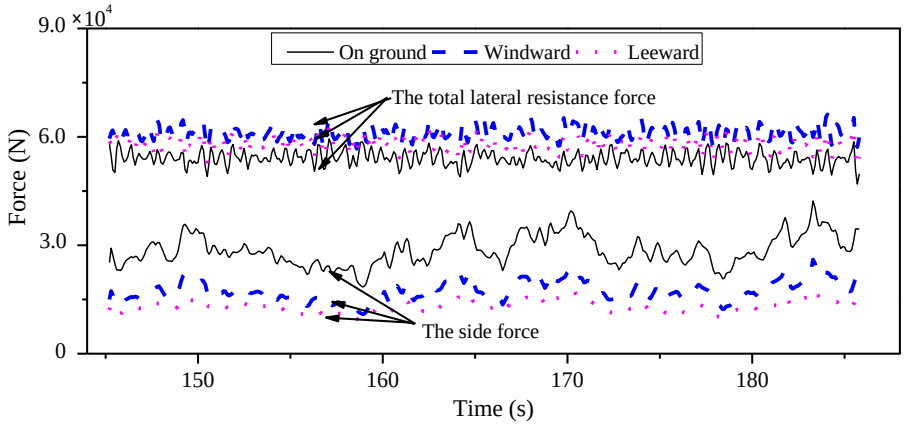

Fig. 12 Side-sliding instability analysis for three different cases

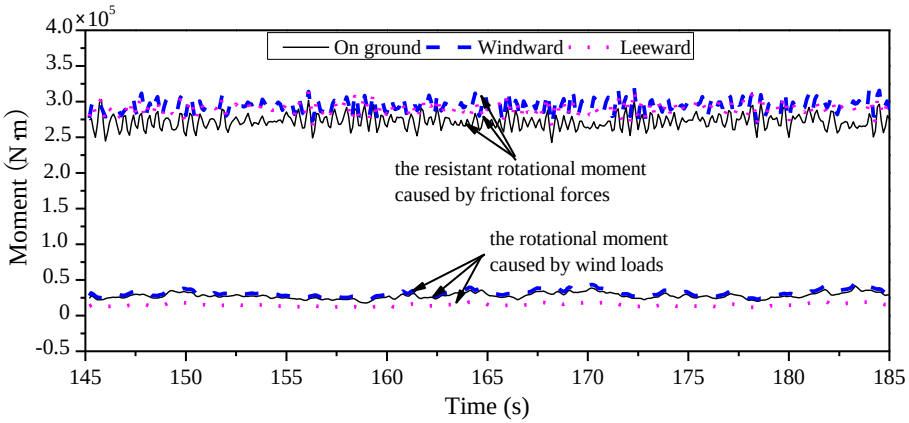

Fig. 13 Rotation instability analysis for three different cases

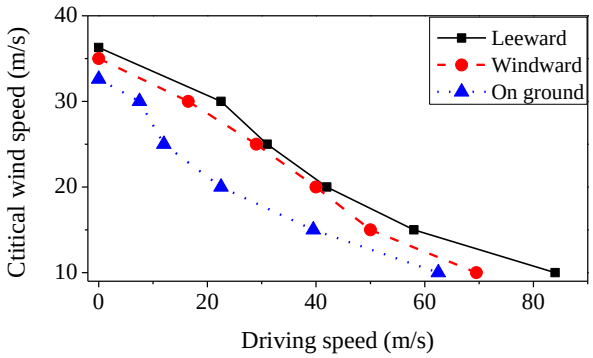

Fig. 14 Critical wind speed versus driving speed under three cases.

4.2.5 Critical wind speed and vehicle acceleration

Overturning, rotation, and side slipping accidents may occur concurrently or sequentially. The critical event is the one that occurs first. The 'critical wind speed' is the highest allowable wind speed under a certain vehicle speed to avoid the risk of a critical accident.

The aerodynamic coefficients have significant and direct influence on the vehicle safety responses as discussed earlier. The accident vehicle speed corresponding to three groups of aerodynamic coefficients under different situations are sought through continuous simulation under a series of vehicle driving speeds. The critical wind speeds versus vehicle driving speeds for the same truck under the three situations can be drawn from the results shown in Fig. 14.

It can be found in Fig. 14 that the vehicle in the leeward lane case has the highest critical wind speed, followed by the vehicle in the windward case, and the third is the vehicle in the ground case. Additionally, there is no significant difference in the allowable wind speed limit between the vehicles on the leeward and windward lanes, whereas the results of both are greater than those on the ground. If the 'critical wind speed' is determined by the aerodynamic coefficients in the ground case, it will be too conservative to maintain high efficiency of traffic operation, which will result in manmade traffic jams and economic loss. Therefore, it is necessary to adopt aerodynamic coefficients considering aerodynamic interference in the WVB analysis.

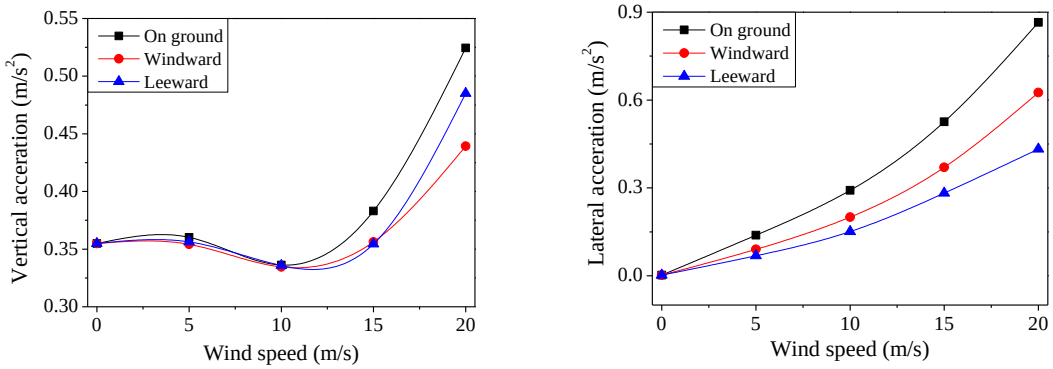

(a) Vertical accelerations (b) Lateral accelerations

Fig. 15 RMS acceleration of vehicle vs. wind velocity (U_v = 80 km/h)

When the vehicle passes the bridge at a speed of 80 km/h, the vertical and lateral standard deviations of the vehicle body accelerations versus wind velocity are shown in Fig. 15. In Fig. 15, the x-axis denotes the mean velocity of the wind speed ranging from 0 to 20 m/s. The findings from Fig. 15 are summarized as follows:

1) When the vehicle travels at 80 km/h under a mean wind speed of 5–10 m/s, the instantaneous attack angles are between 8.83° and 28.47°. The vertical acceleration responses of the vehicle body at these wind speeds under the three situations do not differ significantly. This is due to the slight difference existing in the lift force coefficients when the instantaneous attack angles are between 8.83° to 28.47° as shown in Fig. 7(b). When the wind speed is 15–20 m/s, the instantaneous attack angles range from 24.17° to 50.87°, and the corresponding lift force coefficients in the ground case are greater than those in the bridge deck case. Thus, if adopting the aerodynamic coefficient in the ground case, the vertical acceleration of the vehicle body is apparently greater than those of the windward lane case and the leeward lane case.

2) As shown in Fig. 15(b), the lateral acceleration response of the vehicle body in the ground case is the greatest, the windward lane case is second, and the leeward lane case is the least. This phenomenon is due to a similar relationship to that of the side force coefficients for those three situations as shown in Fig. 7(a).

4.3 The influence of aerodynamic coefficients on the response of the bridge

To investigate the influence of different aerodynamic coefficients on the response of the bridge, the responses of the bridge in cases with different aerodynamic coefficients and wind velocities are chosen in the analysis. Taken aerodynamic parameters as the standard, all the cases can be divided into two categories: the windward and leeward case, and the only two differences between the two cases are the lateral position of vehicles and the aerodynamic coefficients that the vehicles adopted. In the two cases, the same aerodynamic coefficient (Han 2006) is adopted for the bridge. Four wind velocities (5, 10, 15, and 20 m/s) are set up in each case. All cases occur with a vehicle speed of 80 km/h and a yaw angle of 90°. The displacement and acceleration information of the bridge can be extracted directly from the numerical WVB analysis model established in the previous section.

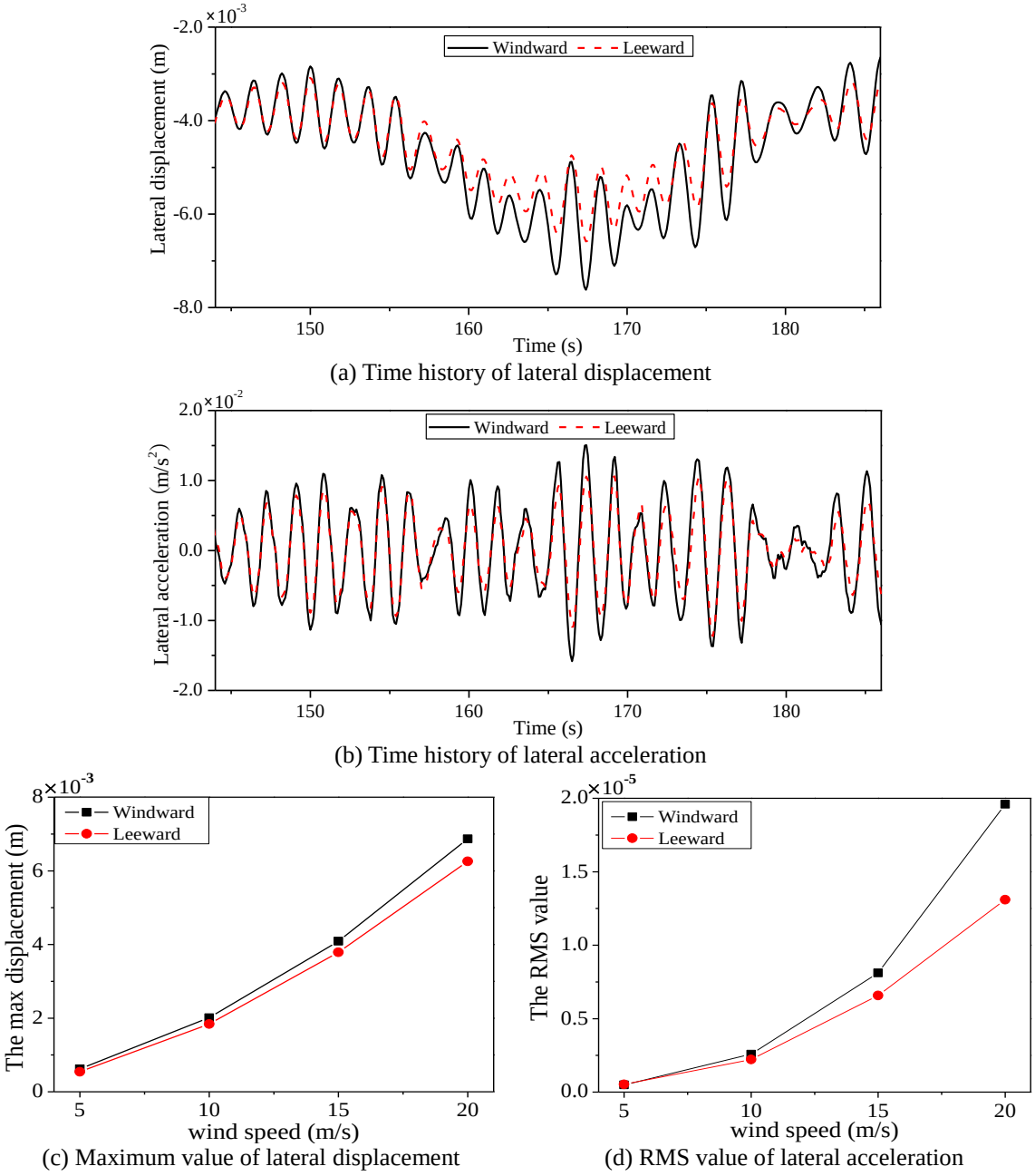

(a) Time history of lateral displacement

(b) Time history of lateral acceleration

(c) Maximum value of lateral displacement

(d) RMS value of lateral acceleration

Fig. 16 Lateral response of bridge girder at mid-span

Fig. 16 shows the response of the bridge mid-span. Figs. 16(a) and 16(b) exhibit the simulated time histories of lateral displacement and acceleration at the mean wind velocity of 20 m/s. The maximum value of lateral displacement and RMS of lateral acceleration at different wind velocities are displayed in Figs. 16(c) and 16(d).

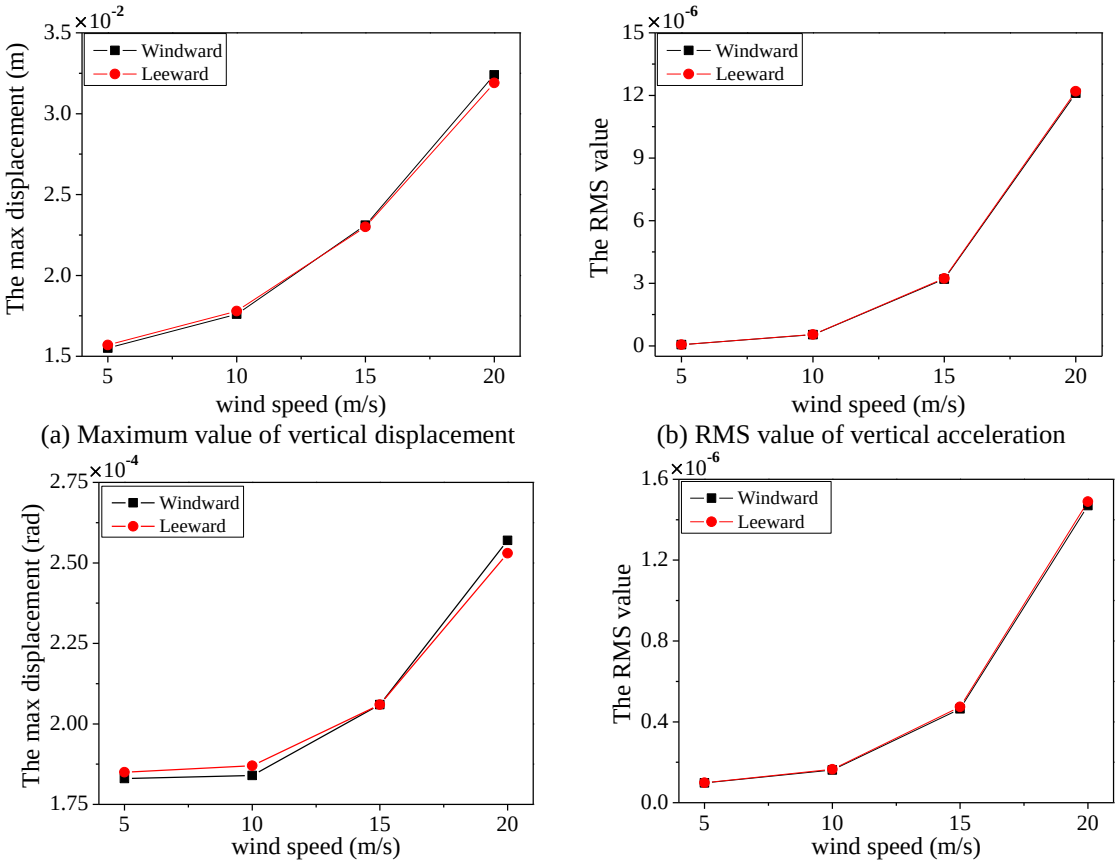

Fig. 17 Vertical and torsional response of bridge girder at mid-span

Based on the observations from Fig. 16, the characteristics of the bridge dynamic performance under different wind velocities and vehicle platoons with different aerodynamic coefficients are summarized as follows:

1) The time history curves of the lateral displacements and acceleration at the mid-span when the vehicle platoon adopts a windward aerodynamic coefficient share the same trend as that of the leeward aerodynamic coefficient, and all curves reach their maximum values as the vehicle platoon approaches the mid-span. When the vehicle platoon adopts the windward aerodynamic coefficient, the fluctuation range is slightly larger than when adopting the leeward aerodynamic coefficient. The maximum lateral displacement and the RMS of acceleration of the bridge mid-span increase rapidly with increasing wind velocity. At every wind velocity, the bridge displacement and acceleration response adopting the windward aerodynamic coefficient are slightly greater than when adopting the leeward aerodynamic coefficient.

2) The lateral displacements and acceleration of the bridge are generated by wind that acts on the vehicle and the bridge, and the wind acting on the bridge plays the main role. For the two cases adopting different aerodynamic coefficients, the wind acting on the bridge is the same, which

causes the lateral time history response curves of the bridge in the two cases to have the same trend and results in a rapid increase in the maximum lateral displacements and the RMS of acceleration of the bridge mid-span with increasing wind velocity. In Fig. 7(a), the windward side force coefficient is greater than the leeward side force coefficient, so the vehicle wind load adopting the windward aerodynamic coefficient is greater. The wind load of the vehicle is transmitted to the bridge, so the bridge lateral response adopting the windward aerodynamic coefficient is slightly greater than that when adopting the leeward aerodynamic coefficient.

Owing to the limited space, Fig. 17 presents only the maximum torsional and vertical displacements and the RMS of the acceleration of the bridge under different wind velocities. In Fig. 17, the following can be observed:

1) Wind has great influence on the dynamic responses of the bridge in the vertical and torsional directions, resulting in the same trend in each group's bridge response, all of which increase rapidly with increasing wind velocity. At every wind velocity, the bridge response is slightly different, which is mainly as a result of aerodynamic force.

2) When the wind speed is less than 10 m/s, the maximum values of vertical displacement and RMS of the vertical acceleration of the bridge adopting the windward coefficient are smaller than those of the leeward case. However, they are greater than the leeward case in the wind speed range from 15 to 20 m/s. When the wind speed is less than 10 m/s, the attack angles reach 28.47°. In Fig. 7, as the attack angle is less than 30°, and the lift force coefficient in the windward case is greater than that of the leeward case. Thus, the vertical lift force of the vehicle platoon adopting the windward coefficient is greater, and the vertical force acting on the bridge produced by the vehicle platoon adopting the windward coefficient is less than that of the leeward case, so the bridge vertical response is smaller. In addition, when the wind speed is between 15 m/s and 20 m/s, the attack angle ranges from 24.17° to 50.87°, and the lift coefficient of the windward case is smaller, leading to a greater response of the bridge than in the leeward case.

3) The bridge torsional response is influenced by not only vertical force but also lateral force, but the vertical force plays the main role, so the torsional response has a similar trend to the vertical response. When the wind speed is less than 10 m/s, the bridge torsional maximum displacement when the vehicle platoon adopts the windward coefficient is less than the leeward coefficient, but it becomes greater when the wind speed is between 15 m/s and 20 m/s. Owing to the joint influence of platoon weight and wind load, the sequence of the RMS value of torsional acceleration is not obvious.

By observing Figs. 16 and 17, it can be found that the influences of the different aerodynamic coefficients on the bridge response are very weak.

5. Conclusions

In this study, the aerodynamic interference of the bridge deck on a high-sided truck has been discussed extensively. A series of wind tunnel tests was conducted first to measure the aerodynamic coefficients of the truck on the ground and on the bridge deck. Through the fully coupled wind–vehicle–bridge computation system, the influence of the aerodynamic interference of the bridge deck on the driving safety and passenger comfort was then investigated under different aerodynamic parameters. The impact of different aerodynamic coefficients on the bridge response was also studied. The main conclusions are summarized as follows.

- An experimental setup was developed to measure the aerodynamic characteristics of a high-sided truck, which could consider the aerodynamic interference between the vehicle and the bridge in a wind tunnel. The aerodynamic coefficients of a high-sided vehicle on both the ground and the bridge deck were then determined to explore the effects of the bridge truck and accessory structures. The experimental results show that the side force and drag force coefficients on the bridge deck decrease relative to the same vehicle on the ground owing to the sheltering effect of the side and central protection rails, and the rolling moment coefficients on the bridge deck are greater than those on the ground, especially for those on the windward lane. The influence of the existence of the bridge deck on the lift force coefficient, pitching moment coefficient, and yawing moment coefficient is irregular.
- Vehicle stability and passenger comfort are closely associated with the aerodynamic coefficients adopted in the analysis of the WVB system. The bridge deck case has higher critical wind speeds and lower lateral acceleration responses of the vehicle body compared with those of the ground case. In general, the existence of the bridge deck and accessory structures can play a positive role in enhancing the performance of vehicle safety and passenger comfort. Therefore, the aerodynamic interference should be considered in the WVB system. This consideration can offer a more reasonable critical wind speed on traffic closure, which helps avoid unnecessary traffic control and improve the efficiency of transportation.
- The time history curves, maximum values and RMS values of the bridge response extracted from the WVB system when vehicle adopts different aerodynamic coefficients at different wind velocities were compared to explore the effect of aerodynamic interference on the bridge response. Although the vehicle platoon adopted different aerodynamic coefficients, the trend of the bridge response is the same because the wind acting on the bridge plays the main role in generating the bridge response regardless of vertical, lateral and torsional directions. At every wind velocity, the platoons adopting different aerodynamic coefficients resulted in different bridge responses, but the differences were very slight. The influence of aerodynamic interference has little effect on the response of the bridge.

Acknowledgements

This research is supported by the National Science Foundation of China (Project No. 51278064, 51108154 and 51408053) and the Fundamental Research Funds for the Central Universities (310821162008). The opinions, findings and conclusions expressed are those of the writers and do not necessarily present the views of the sponsors.

References

Baker, C.J. (1991), "Ground vehicles in high cross winds part 1: steady aerodynamic forces", *J. Fluid. Struct.*, **5**(1), 69-90.

Baker, C.J. (1994), "The quantification of accident risk for road vehicles in cross winds." *J. Wind Eng. Ind. Aerod*., **52**, 93-107.

Baker, C.J. and Reynolds, S. (1992), "Wind induced accidents of road vehicles", *Accid. Anal. Prev.*, **24**(6), 559-575.

Bettle, J., Holloway, A.G.L. and Venart, J.E.S. (2003), "A computational study of the aerodynamic forces

acting on a tractor-trailer vehicle on a bridge in cross-wind", *J. Wind Eng. Ind. Aerod.*, **91**(5), 573-592.
Cai, C.S. and Chen, S.R. (2004), "Framework of vehicle-bridge-wind dynamic analysis." *J. Wind Eng. Ind. Aerod.*, **92**, 579-607.
Chen, S.R. and Cai, C.S. (2004), "Accident assessment of vehicles on long-span bridges in windy environments", *J. Wind Eng. Ind. Aerod*., **92**(12), 991-1024.
Cheung, M.S. and Chan, Y.B. (2010), "Operational requirements for long span bridges under strong wind events", *J. Bridge Eng.*, **15**(2), 131-143.
Davenport, A.G. (1968), "The dependence of wind load upon meteorological parameters", *Proceedings of the International Research Seminar on Wind Effects on Building and Structures*, University of Toronto Press, Toronto, 19-82.
Guo, W.H. and Xu, Y.L.(2006), "Safety analysis of moving road vehicles on a long bridge under crosswind." *J. Eng. Mech.*, **132**(4), 438-446.
Han, W.S. (2006), *Three-dimensional coupling vibration of wind-vehicle-bridge system*, Ph.D. Dissertation, Tongji University, Shanghai, (in Chinese).
Han, W.S., Ma, L., Cai, C.S., Chen, S.R. and Wu, J. (2015a), "Nonlinear dynamic performance simulation of super-Long-Span cable-stayed bridge under traffic and wind", *Wind Struct.*, **20**(2), 249-274.
Han, W.S., Wu, J., Cai, C.S. and Chen, S.R. (2015b), "Characteristics and dynamic impact of overloaded extra heavy trucks on typical highway bridges", *J. Bridge Eng.*, **20**(2), 315-331.
Han, Y., Cai, C.S., Zhang, J. R., Chen, S.R. and He, X.H. (2014), "Effects of aerodynamic parameters on the dynamic responses of road vehicles and bridges under cross winds", *J. Wind Eng. Ind. Aerod*., **134**, 78-95.
Han, Y., Chen, H., Shen, L. and Cai, C.S. (2015), "Effects of aerodynamic parameters on coupled dynamic responses of wind-vehicle-bridge system", *Chin. J. Highw. Transport*, **28**(9), 57-66,126.
Han, Y., Hu, J.X., Cai, C.S., Chen, Z.Q. and Li, C.G. (2013), "Experimental and numerical studies of aerodynamic forces on vehicles and bridges", *Wind Struct.*, **17**(2), 163-184.
International Organization for Standardization (ISO). (1995), "*Mechanical Vibration-Road Surface Profiles-Reporting of measured Data*", ISO 8068:(E), ISO, Geneva.
Kaimal, J.C., Wyngaard, J.C., Izumi, I. and Cote, O.R. (1972), "Spectral characteristics of surface-layer tursbulence", *Q. J. Roy. Meteorol. Soc.*, **98**(417), 563-589.
Li, Y., Lu, D.G. and Sheng, H.F. (2012), "Fatigue reliability analysis on cable of cable-stayed bridge under random vehicle load and wind load", *Chin. J. Highw. Transport*, **25**(2), 60-67.
Li, Y.L., Zhao, K., Chen, N. and Liao, H.L. (2012), "Wind-vehicle-bridge system coupling vibration and traffic safety analysis", *Eng. Mech*., **29**(5), 206-212.
Lumley, J.L. and Panofsky, H.A. (1964), *The Structure of Atmospheric Turbulence*, Wiley, New York.
Ma, L., Han, W.S., Ji, B.H. and Liu, J.X. (2015), "Probability of overturning for vehicles moving on a bridge deck in a wind environment considering stochastic process characteristics of excitations", *J. Perform. Constr. Fac.*, **29**(1), 249-274.
Society of Automotive Engineers (SAE). (1993), "*Aerodynamic testing of road vehicles: Testing methods and procedures.*" SAE Standards, Aerodynamics, Product Code, J2084-199301.
Suzuki, M., Tanemoto, K. and Maeda, T. (2003), "Aerodynamic characteristics of train/vehicles under cross winds", *J. Wind Eng. Ind. Aerod.*, **91**(1-2), 209-218.
Wang, B., Xu, Y.L. and Li, Y.L. (2015), "Dynamic analysis of wind-vehicle-bridge systems using mutually-affected aerodynamic parameters", *Wind Struct*., **20**(2), 191-211.
Wang, T., Han, W.S., Yang, F. and Kong, W. (2014), "Wind-vehicle-bridge coupled vibration analysis based on random traffic flow simulation." *J. Traffic Transp. Eng. (Engl. Ed.)*, **1**(4), 293-308.
Wu, Y.Z. (2008), *Research on Automotive Aerodynamic Characteristics during Overtaking*, Ph.D. Dissertation, Ji Lin University, Changchun, (in Chinese).
Xu, W.N. and Shi, R.G. (2002), "*Design Wind Speed Calculation and Gradient Wind Speed Observation of Hangzhou Gulf Bridge*", Ning bo Weather Center, Ningbo, China.
Xu, Y.L. and Guo, W.H. (2003), "Dynamic analysis of coupled highway vehicle and cable-stayed bridge systems under turbulent wind", *Eng. Struct.*, **25**(4), 473-486.
Zhu, L.D., Li, L., Xu, Y.L. and Zhu, Q. (2012), "Wind tunnel investigations of aerodynamic coefficients of

road vehicles on bridge deck", *J. Fluids Struct.*, **30**(2), 35-50.

AD